isvr Institute of Sound and Vibration Research

# Energy Distribution Approach, Energy Influence Coefficients and Asymtotic Scaled Modal Analysis

**S. De Rosa and B. R. Mace**

ISVR Technical Memorandum No 963

May 2006

University of Southampton

# SCIENTIFIC PUBLICATIONS BY THE ISVR

***Technical Reports*** are published to promote timely dissemination of research results by ISVR personnel. This medium permits more detailed presentation than is usually acceptable for scientific journals. Responsibility for both the content and any opinions expressed rests entirely with the author(s).

***Technical Memoranda*** are produced to enable the early or preliminary release of information by ISVR personnel where such release is deemed to the appropriate. Information contained in these memoranda may be incomplete, or form part of a continuing programme; this should be borne in mind when using or quoting from these documents.

***Contract Reports*** are produced to record the results of scientific work carried out for sponsors, under contract. The ISVR treats these reports as confidential to sponsors and does not make them available for general circulation. Individual sponsors may, however, authorize subsequent release of the material.

# Energy Distribution Approach, Energy Influence Coefficients and Asymptotic Scaled Modal Analysis

**S. De Rosa and B.R. Mace**

ISVR Technical Memorandum No: 963

May 2006

UNIVERSITY OF SOUTHAMPTON

INSTITUTE OF SOUND AND VIBRATION RESEARCH

DYNAMICS GROUP

# Energy Distribution Approach, Energy Influence Coefficients and Asymptotic Scaled Modal Analysis

by

**S. De Rosa and B.R. Mace**

ISVR Technical Memorandum No: 963

May 2006

Authorised for issue by
Professor M.J. Brennan
Group Chairman

Table of Contents

Table of Figures

## 1. Introduction

Inside the large field of structural dynamic and vibroacoustic predictive methodologies, the **Energy Influence Coefficient** (EIC) and the **Energy Distribution Approach** (EDA) represent theoretical and numerical tools which have appeared in recent times, ref.[1÷3]. In fact, by using the global modes of the system under investigation, it was possible to define all the relevant energies and powers as used in standard energy methods. Among these, the most popular is **Statistical Energy Analysis** (SEA), ref.[4].

EDA is a theoretical frame in which it is possible to find a link between the deterministic modal methods and the energy ones. Further, it is well known that the validity of some SEA approximations and assumptions are not known *a priori*, while adopting EDA and EIC, it is possible to check the conditions in which a *proper* SEA model could be assembled, ref.[3,5].

In SEA, for example, the coupling loss factors are strictly positive, and further they are zero for indirectly coupled subsystems. By using EDA, it was demonstrated that the indirect coupling loss factors can exist and they can be negative. Clearly, in this condition the system cannot be modelled with standard SEA approach, ref.[6].

At the same time, a novel approach was studying the possibility to use finite element approach (FEA) for getting the *high frequency* response (the response of a given system at high values of the modal overlap factors), ref.[6÷9]. A scaling procedure was tailored in order to get the same energy representation by using a reduced modal base.

This can be done (i) to reduce the computational costs for given prediction at a given frequency range, or (ii) for increasing the frequency range for which the model is valid for the same computational cost. It is not worth noting that the cost of the FEA is associated with the ratio of the wavelength to the dimensions of the structure.

An acceptable justification of the scaling procedure was found by using SEA approach, but only with EDA (and EIC) it was possible to properly frame all the relevant parameters, ref.[10].

The results obtained for several assemblies demonstrated that the scaling procedure, named **Asymptotical Scaled Modal Analysis** (ASMA), was able to predict the response in an SEA sense by using a scaled model with standard **Finite Element Approach** (FEA) and model, ref.[11].

The contents of this report concerns various applications of ASMA in the context of EDA/EIC and they are closely related to ref.[5], in which the analysis was focused on estimating the coupling loss factors from FEA in a robust approach.

The results herein presented and discussed, have demonstrated that ASMA is able to furnish the coupling loss factors at reduced computational cost when compared with the standard analysis.

## 2. Energy Distribution Approach, Energy Influence Coefficients and Asymptotic Scaled Modal Analysis

### 2.1 Review of Energy Distribution Approach

Full details can be found in ref.[1, 2 and 3]. In summary, the structure is analyzed using FEA, for example, and the modes found. The discrete frequency response at a point can be found for point force excitation by summing contributions from the modes in a conventional manner. This response is then measured to find relations between the input power and the energies.

First, the mean square velocity response (which is proportional to the kinetic energy) in a subsystem is found by integrating the point response over the region occupied by the subsystem.

Next, rain-on-the-roof excitation is assumed: this is spatially delta-correlated. By averaging the energy response for all possible excitation points in a given subsystem, the total response energy is found. This can then be frequency averaged. Next, the subsystem input power is found by integrating the real part of input velocity response to point force excitation over the region occupied by the excited subsystem and over frequency. Finally, the energy influence coefficients (EIC) are found: these are simply the subsystem energies per unit input power.

Then, EDA involves post-processing the results of a modal analysis typically performed using FEA of the whole structure. This poses the problems at high frequencies of the large computational costs that might be associated with the FEA.

This report describes how ASMA might be used to scale the structure, perform the FEA on the scaled structure at low cost, and have estimate of the EICs. It is necessary, therefore, that the modes of the scaled systems, when suitably averaged, resemble the same average of the modes of the original system.

### 2.2 Justification of the Asymptotic Scaled Modal Analysis by using Energy Distribution Approach

This paragraph has been extracted from ref.[10] and added here for sake of completeness.

In ASMA a scaled model of the original system is analysed. The given original model is geometrically scaled by multiplying the side dimensions of the original model by the factor $\sigma<1$, so that a FE model becomes correspondingly smaller and the modal density decreases.

In particular the natural frequencies of the model scale as (for plates):

$$\overline{\omega}_j = \sigma^{-2}\omega_j \tag{1}$$

where the overbar denotes a scaled quantity. The model is also scaled dynamically, to retain similar modal characteristics. For example, the damping loss factor is increased by the factor $\varepsilon$ ($\varepsilon<1$) so that:

$$\overline{\eta}_j = \varepsilon^{-1}\eta_j \tag{2}$$

At this stage, we also assume that the forcing function is the same for both the original and scaled structures. In the EDA approach, the energy response is defined in terms of the following parameters which depend on the modal properties of the system ref.[1].

First, the original and the scaled parameters

$$\psi_{jk}^{(r)} = \int_{x\in r} \rho(x)\phi_j(x)\phi_k(x)dx \qquad \overline{\psi}_{pq}^{(\bar{r})} = \int_{x\in \bar{r}} \overline{\rho}(x)\overline{\phi}_p(x)\overline{\phi}_q(x)dx \tag{3}$$

depend on the global mode shapes within the original, r, and scaled, $\bar{r}$ ,subsystems. Specifically, the subscripts j and k refer to the global mode shapes of the original model and the subscripts p and q refer to the global mode shapes of the scaled one. If properly scaled the statistics of $\psi_{jk}^{(r)}$ can be approximated by the scaled modes, that is $\psi_{jk}^{(r)} \cong \overline{\psi}_{pq}^{(\bar{r})}$. The coordinate x is the position vector in a one, two or three-dimensional structure and ρ(x) is the mass density.

Secondly the auto and cross-modal frequency response operators, ref.[1], for the original and scaled systems are as follows:

$$\Gamma_{jj} = \frac{1}{\Omega}\frac{\pi}{8\eta_j\omega_j}; \qquad \overline{\Gamma}_{jj} = \frac{1}{\Omega}\frac{\pi}{8\overline{\eta}_j\,\overline{\omega}_j} = \frac{1}{8\Omega}\frac{\pi}{\frac{\eta_j}{\varepsilon}\frac{\omega_j}{\sigma^2}} = \varepsilon\sigma^2\Gamma_{jj} \tag{4}$$

The original cross modal frequency response operators are:

$$\Gamma_{jk} = \frac{\pi}{16\Omega}\frac{\left(\omega_j+\omega_k\right)^2\left(\eta_j\omega_j+\eta_k\omega_k\right)}{\left(\omega_j^2-\omega_k^2\right)^2+\left(\eta_j\omega_j^2+\eta_k\omega_k^2\right)^2} \tag{5-a}$$

The scaled cross modal frequency response operators are:

$$\overline{\Gamma}_{jk} = \frac{\pi}{16\Omega}\frac{\left(\overline{\omega}_j+\overline{\omega}_k\right)^2\left(\overline{\eta}_j\,\overline{\omega}_j+\overline{\eta}_k\,\overline{\omega}_k\right)}{\left(\overline{\omega}_j^2-\overline{\omega}_k^2\right)^2+\left(\overline{\eta}_j\,\overline{\omega}_j^2+\overline{\eta}_k\,\overline{\omega}_k^2\right)^2} = \frac{\pi}{16\Omega\sigma^4\sigma^2\varepsilon}\frac{\left(\omega_j+\omega_k\right)^2\left(\eta_j\omega_j+\eta_k\omega_k\right)}{\frac{\left(\omega_j^2-\omega_k^2\right)^2}{\sigma^8}+\frac{\left(\eta_j\omega_j^2+\eta_k\omega_k^2\right)^2}{\sigma^8\varepsilon^2}} \tag{5-b}$$

$$= \frac{\pi}{16}\frac{\varepsilon\sigma^2}{\Omega}\frac{\left(\omega_j+\omega_k\right)^2\left(\eta_j\omega_j+\eta_k\omega_k\right)}{\varepsilon^2\left(\omega_j^2-\omega_k^2\right)^2+\left(\eta_j\omega_j^2+\eta_k\omega_k^2\right)^2}$$

The term Ω represents a generic frequency band over which excitation is applied. The cross modal terms are not yet scaled since the quantities involved are different functions of σ and ε. Thus it is mandatory to work with approximations for these terms.

For ***large terms***, which broadly represent the interaction of two overlapping modes, one gets:

$$\overline{\Gamma}_{jk_{large}} \cong \frac{\pi\sigma^2}{16\Omega}\frac{\left(\omega_j+\omega_k\right)^2\left(\eta_j\omega_j+\eta_k\omega_k\right)}{\varepsilon}\left[\frac{\left(\eta_j\omega_j^2+\eta_k\omega_k^2\right)^2}{\varepsilon^2}\right]^{-1} = \varepsilon\sigma^2\Gamma_{jk_{large}}. \tag{6}$$

It should be noted that the *scaled large terms* are ruled by ε and $\sigma^2$ as the terms $\overline{\Gamma}_{jj}$, Eq.(4).

For ***small terms*** (broadly, modes which do not overlap) one gets:

$$\overline{\Gamma}_{jk\,small} \cong \frac{\pi}{16\Omega}\frac{\left(\overline{\omega}_j+\overline{\omega}_k\right)^2\left(\overline{\eta}_j\,\overline{\omega}_j+\overline{\eta}_k\,\overline{\omega}_k\right)}{\left[\left(\overline{\omega}_j^2-\overline{\omega}_k^2\right)^2\right]}=\frac{\pi\varepsilon\sigma^2}{16\Omega}\frac{\left(\omega_j+\omega_k\right)^2\left(\eta_j\omega_j+\eta_k\omega_k\right)}{\left[\left(\omega_j^2-\omega_k^2\right)^2\varepsilon^2\right]}=\frac{\sigma^2}{\varepsilon}\Gamma_{jk\,small}. \qquad (7)$$

This is the central point of the scaling procedure.

The small coupling terms are the only ones that do not follow the scaling rule of $\sigma^2\varepsilon$. The scaling coefficients are both less than unity, the circumstances under which the approximation for $\sigma^2\,\varepsilon^{-1}$ can be a good estimate of $\sigma^2\varepsilon$ have to be borne in mind. It can be shown that the best approximation is obtained when selecting $\varepsilon = \sigma$. In this case the small terms for the coupling are an acceptable first order approximation around unity.

Expanding around $\sigma$=1 gives:

$$\begin{aligned}&\text{for the large terms}: \ \sigma^3 \cong 1+\left(3\sigma^2\right)_{\sigma=1}(\sigma-1)=3\sigma-2;\\ &\text{for the small terms}: \frac{\sigma^2}{\varepsilon}=\sigma\end{aligned} \quad . \qquad (8)$$

It is trivial to note that for $\varepsilon=\sigma=1$ one gets the original system. Furthermore, for the response of a single subsystem and/or the directly excited subsystem drawn from a generic assembly, any choice for $\sigma$ could be used. It is useful to underline again that approximations for the *small modal coupling terms* are solely responsible for ASMA not being an *exact* translation of the energy content at high frequencies.

### 2.3 Summary of Asymptotic Scaled Modal Analysis

The application of the scaling procedure leads to the analysis of the auto and cross modal frequency response operators.

The auto modal frequency operators, $\Gamma_{jj}$, result in a scaling as $\varepsilon\sigma^2$, Eq.(4).

The cross modal ones, $\Gamma_{jk}$, result in a complicated dependence on $\sigma$ and $\varepsilon$, Eq.(5), which can be treated only by invoking some approximations, Eq.(6) and Eq.(7). The *large* cross modal terms follow the $\varepsilon\sigma^2$ scaling law, Eq.(6), while the *small* ones are scaled with $\varepsilon^{-1}\sigma^2$. The best scaling is obtained by selecting $\varepsilon=\sigma$; in this case, the small cross modal terms can be used as an acceptable approximation.

The auto modal frequency operators, $\Gamma_{jj}$, are the parameters that govern the input power, that is the amount of energy entering the given subsystem and, therefore, it is expected that ASMA might always work well for such system components.

It is also expected that the energy exchange between the remaining subsystems (not directly excited) will be well approximated, these being dominated by the largest cross modal frequency operators, $\Gamma_{jk}$, since they result from those modes that overlap.

The results presented in the next paragraph will confirm these statements based on theoretical considerations.

The parameters required are as follows. The original and scaled power input in the s-th subsystem are:

$$\begin{aligned} P_{IN}^{(s)} &= 2S_f \sum_j 2\eta_j \omega_j \Gamma_{jj} \psi_{jj}^{(s)} \\ \overline{P}_{IN}^{(s)} &= 2S_f \sum_j 2\overline{\eta}_j \overline{\omega}_j \overline{\Gamma}_{jj} \overline{\psi}_{jj}^{(s)} = 2S_f \sum_j 2\left(\frac{\eta_j}{\varepsilon}\right)\left(\frac{\omega_j}{\sigma^2}\right)\left(\varepsilon\sigma^2\Gamma_{jj}\right)\left(\psi_{jj}^{(s)}\right) = P_{IN}^{(s)} \end{aligned} \tag{9}$$

It has to be noted that the spatial distribution of the excitation acting in a frequency band has to be considered; in ref.[1], the loading was assumed to be proportional to mass density with a zero cross-spectral density and an auto-spectral density, $S_f$.

The original and scaled kinetic energies for the r-th subsystem are:

$$\begin{aligned} T^{(r)} &= 2S_f \sum_j \sum_k \Gamma_{jk} \psi_{jk}^{(s)} \psi_{jk}^{(r)} \\ \overline{T}^{(r)} &\cong 2S_f \sum_j \sum_k \left(\varepsilon\sigma^2\Gamma_{jk}\right)\left(\psi_{jk}^{(s)}\right)\left(\psi_{jk}^{(r)}\right) = \varepsilon\sigma^2 T^{(r)} = \sigma^3 T^{(r)} \end{aligned} \tag{10}$$

The original and scaled energy coefficients are:

$$A_{rs} = \frac{\sum_j \sum_k \Gamma_{jk} \psi_{jk}^{(s)} \psi_{jk}^{(r)}}{\sum_j \eta_j \omega_j \Gamma_{jj} \psi_{jj}^{(s)}}; \qquad \overline{A}_{rs} = A_{rs}\varepsilon\sigma^2 = A_{rs}\sigma^3 \tag{11}$$

while the original and scaled mean square velocities become:

$$v^2 = \frac{T^{(r)}}{m}; \qquad \overline{v}^2 = \frac{\overline{T}^{(r)}}{\overline{m}} = \frac{\sigma^2\varepsilon T^{(r)}}{\sigma^2 m} = \varepsilon\frac{T^{(r)}}{m} = \sigma v^2 \tag{12}$$

The $A_{rs}$ coefficients form a matrix A that under some condition is the inverse of the SEA predictive one (the matrix formed by the direct and coupling loss factors), ref.[1]. The mean square excitation in a band $\delta\omega$ can be generically written as follows, $\frac{1}{2}\left|F^2\right| = S_f(\omega)\rho(x)\delta\omega$.

For the configurations herein introduced and analyzed in the next sections, the same loading function has been assumed for both the original and scaled assembly expansions. This leads to an auto spectral density, $\sigma^{-2}\, S_f(\omega)$ in the scaled system.

The Eqs.(9 to 13) can be summarised as:

$$\overline{S}_f = S_f \Rightarrow \begin{cases} \overline{P}_{IN}^{(s)} = P_{IN}^{(s)} \\ \overline{T}^{(r)} = \sigma^3 T^{(r)} \\ \overline{A}_{rs} = A_{rs}\sigma^3 \\ \overline{v}^2 = \dfrac{\overline{T}^{(r)}}{\overline{m}} = \dfrac{\sigma^3 T^{(r)}}{\sigma^2 m} = \dfrac{\sigma T^{(r)}}{m} = \sigma v^2 \;\Rightarrow\; v^2 = \dfrac{\overline{v}^2}{\sigma} \end{cases} \tag{13-a}$$

$$\overline{S}_f = \sigma^{-2} S_f \Rightarrow \begin{cases} \overline{P}_{IN}^{(s)} = \sigma^{-2} P_{IN}^{(s)} \\ \overline{T}^{(r)} = \sigma T^{(r)} \\ \overline{A}_{rs} = A_{rs}\sigma^3 \\ \overline{v}^2 = \dfrac{\overline{T}^{(r)}}{\overline{m}} = \dfrac{\sigma T^{(r)}}{\sigma^2 m} = \dfrac{T^{(r)}}{\sigma m} = \sigma^{-1} v^2 \quad \Rightarrow \quad v^2 = \sigma \overline{v}^2 \end{cases} \tag{13-b}$$

## 3. A Simple Plate in Bending

The model under analysis is a simple flexural plate. The material plate is homogenous, isotropic and the side lengths are $L_x$ and $L_y$; the thickness is denoted by h. The plate is simply supported along the edges (zero displacements and moments and allowed rotations). The scaling procedure is applied to the analytical solution, by reducing the side dimension by the factor $\sigma$ ($\sigma<1$) and keeping the original thickness. The material is aluminium and has a normal modulus of elasticity, E, and mass density, $\rho$. These are the values in the scaled model, too.

It is useful to report each part of the original and scaled plates. The scaled items are denoted by an overbar. The dimensions are

$$\overline{L}_x = L_x\sigma;\ \overline{L}_y = L_y\sigma;\ \overline{h} = h \tag{14}$$

The natural frequencies in rad/sec are:

$$\begin{aligned} \omega_j &= \sqrt{\frac{Eh^2}{12\rho(1-\nu^2)}}\left[\left(\frac{j_x\pi}{L_x}\right)^2 + \left(\frac{j_y\pi}{L_y}\right)^2\right] \\ \overline{\omega}_j &= \sqrt{\frac{Eh^2}{12\rho(1-\nu^2)}}\left[\left(\frac{j_x\pi}{L_x\sigma}\right)^2 + \left(\frac{j_y\pi}{L_y\sigma}\right)^2\right] = \frac{\omega_j}{\sigma^2} \end{aligned}; \tag{15}$$

and the associated mode shapes:

$$\begin{aligned} \phi_j(x,y) &= \sqrt{\frac{4}{\rho L_x L_y h}}\sin\left(\frac{j_x\pi x}{L_x}\right)\sin\left(\frac{j_y\pi y}{L_y}\right) \\ \overline{\phi}_j(\overline{x},\overline{y}) &= \sqrt{\frac{4}{\rho \overline{L}_x \overline{L}_y h}}\sin\left(\frac{j_x\pi\overline{x}}{\overline{L}_x}\right)\sin\left(\frac{j_y\pi\overline{y}}{\overline{L}_y}\right) = \frac{1}{\sigma}\phi_j(x,y) \end{aligned}. \tag{16}$$

The integers $j_x$ and $j_y$ indicate the number of half wavelengths on each axis. The modes are both mass normalised, in fact the non zero terms of the diagonal mass matrix are the following:

$$\begin{aligned} m_{gen} &= \rho h\int_0^{L_x}\int_0^{L_y}\phi_j^2(x,y)\,dydx = \frac{4}{L_x L_y}\int_0^{L_x}\int_0^{L_y}\sin\left(\frac{j_x\pi x}{L_x}\right)^2\sin\left(\frac{j_y\pi y}{L_y}\right)^2 dydx = 1 \\ \overline{m}_{gen} &= \rho h\int_0^{\overline{L}_x}\int_0^{\overline{L}_y}\overline{\phi}_j^2(\overline{x},\overline{y})\,dydx = \frac{4}{\overline{L}_x \overline{L}_y}\int_0^{\overline{L}_x}\int_0^{\overline{L}_y}\sin\left(\frac{j_x\pi\overline{x}}{\overline{L}_x}\right)^2\sin\left(\frac{j_y\pi\overline{y}}{\overline{L}_y}\right)^2 dydx = 1 \end{aligned} \tag{17}$$

It is of interest to see the distribution of the original and scaled natural frequencies. This is shown of the Fig.1, in which it is evident the shift due to the scaling coefficient by the factor $\sigma$.

Figure 1: Original and Scaled (σ=0.45) Natural Frequencies [Hz]

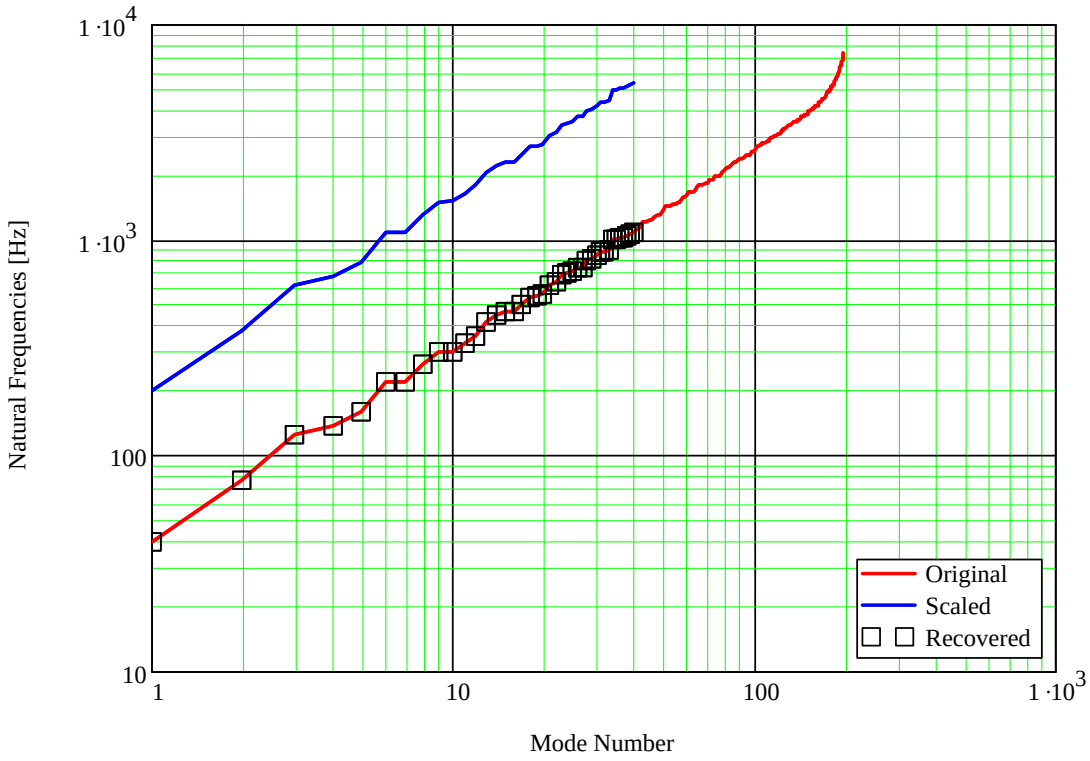


By using an increase of the original damping:

$$\overline{\eta} = \eta\varepsilon^{-1} = \eta\sigma^{-2} \tag{18}$$

it is straightforward to get the results in Fig.2 and 3, where the Classical Modal Analysis (CMA) and Asymptotic Scaled Modal Analysis have been applied in order to get the original and scaled responses, respectively, ref.[10].

The results are expressed in terms of mean square velocity averaged over the acquisition and excitation locations. Further, in those figures, the frequency at which the modal overlap reaches the unit value is also shown.

Figure 2: Original and Scaled Responses with σ=0.45

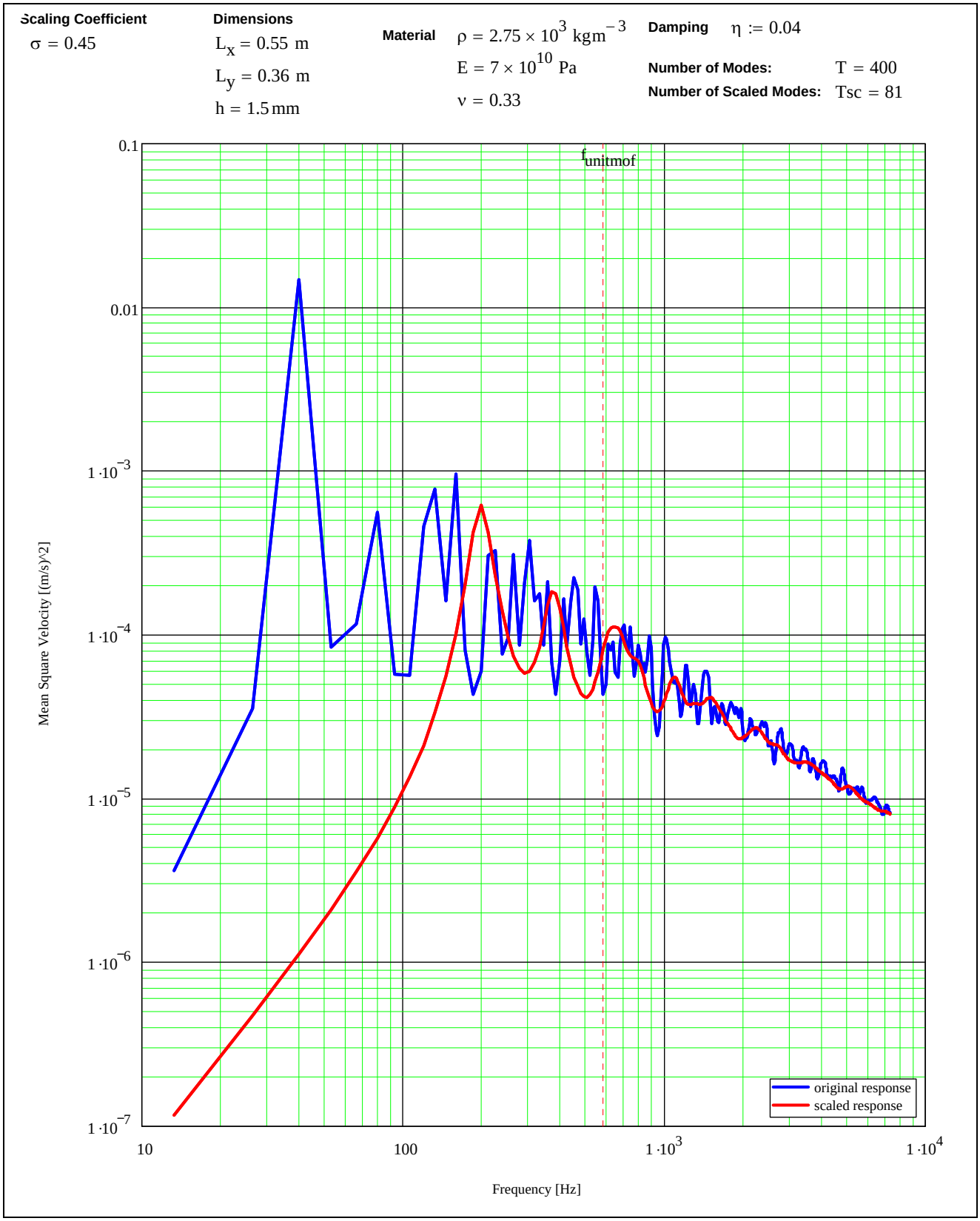

Figure 3: Original and Scaled Responses with σ=0.35

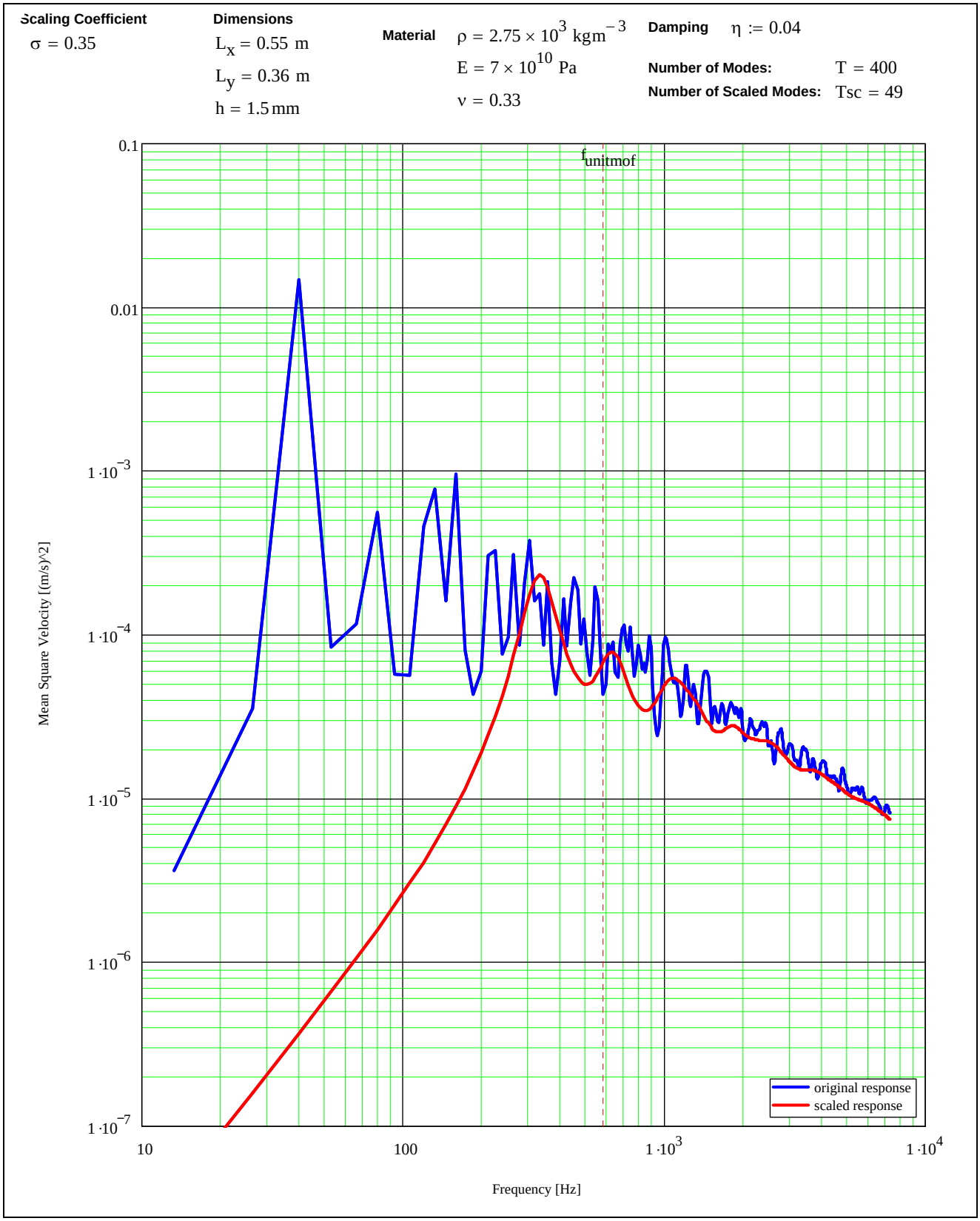

Now, the parameters of the Energy Distribution Approach (EDA) are introduced and discussed. Having selected the normalization of the eigenvectors to give a unit modal mass, the mode shape parameters, $\psi_{jj}$, become:

$$\psi_{jj} = \rho h \int_A \phi_j(x,y)\phi_j(x,y)dxdy = \frac{4}{L_x L_y}\int_0^{L_y}\int_0^{L_x} \sin\left(\frac{j_x \pi x}{L_x}\right)^2 \sin\left(\frac{j_y \pi y}{L_y}\right)^2 dxdy = 1;\ \psi_{jk} = 0$$

$$\overline{\psi}_{jj} = \rho h \int_{\bar{A}} \overline{\phi}_j(\bar{x},\bar{y})\overline{\phi}_j(\bar{x},\bar{y})dxdy = \frac{4}{\bar{L}_x \bar{L}_y}\int_0^{\bar{L}_y}\int_0^{\bar{L}_x} \sin\left(\frac{j_x \pi \bar{x}}{\bar{L}_x}\right)^2 \sin\left(\frac{j_y \pi \bar{y}}{\bar{L}_y}\right)^2 dxdy = 1;\ \overline{\psi}_{jk} = 0 \quad (19)$$

These are interesting results since the terms $\psi_{jj}$ represent the fractional modal density: in this case, they are unity in both the original and scaled models, as expected, and only their distribution along the frequency axis is modified, Fig.4.

Figure 4: The Original and Scaled ($\sigma$=0.45) Terms $\psi_{jj}$ (Original Modes=198, Scaled Modes=40)

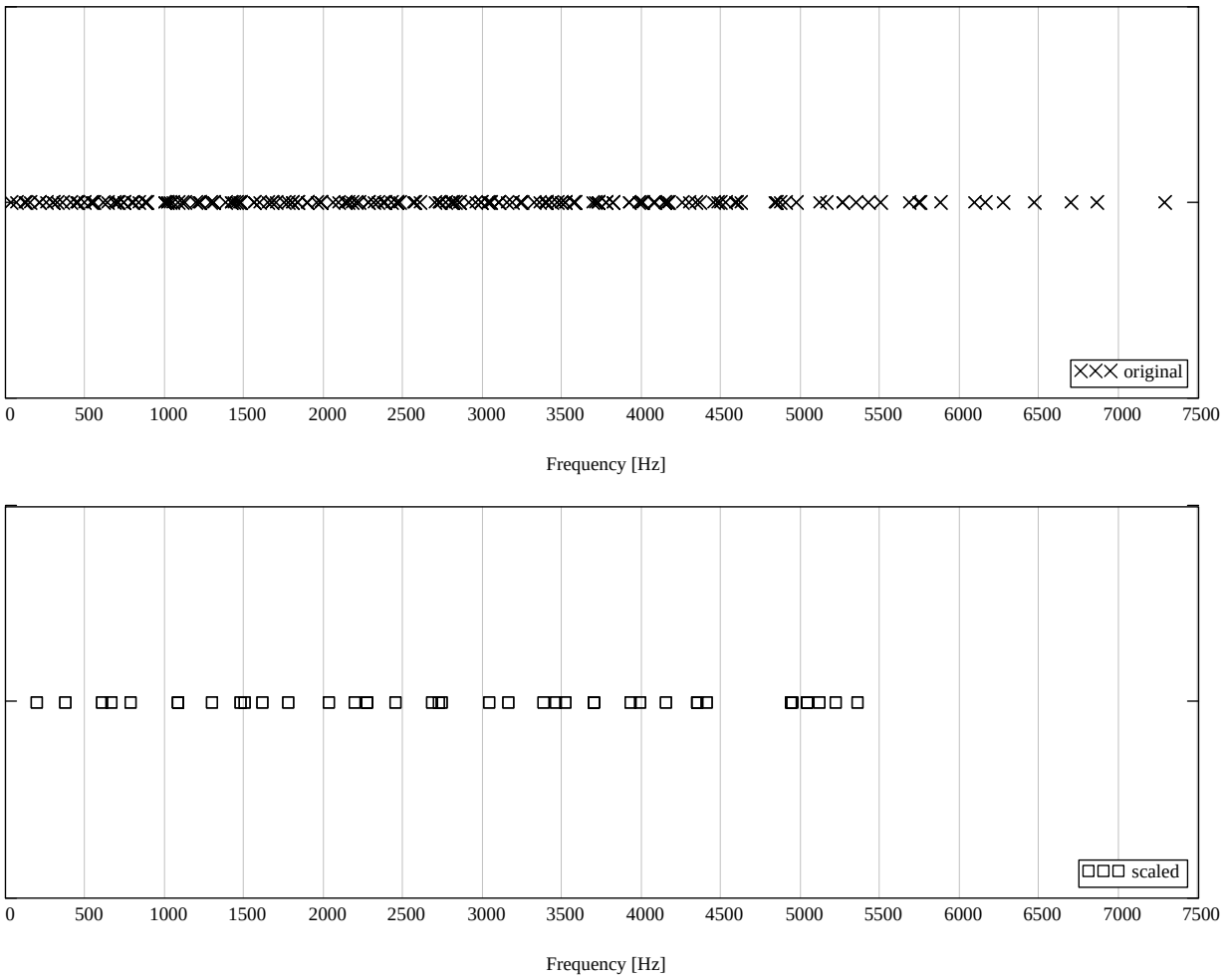


In fact in this simple case, ref.[1]:

$$E[\psi_{jj}^{(s)}] = \nu_s = n_s / n_{TOT} = 1 \quad (20)$$

The modal densities:

$$n_\omega = \frac{\sqrt{3}L_x L_y}{2\pi h\sqrt{\frac{E}{\rho(1-\nu^2)}}}; \quad \overline{n}_\omega = \frac{\sqrt{3}\overline{L}_x \overline{L}_y}{2\pi h\sqrt{\frac{E}{\rho(1-\nu^2)}}} = \sigma^2 n_\omega \tag{21}$$

The modal overlap factors:

$$m_\omega = \omega\eta n_\omega; \quad \overline{m}_\omega = \omega\overline{\eta}\,\overline{n}_\omega = \omega\frac{\eta}{\sigma^2}\sigma^2 n_\omega = m_\omega \tag{22}$$

If the damping is small, ref.[1] and previous paragraph, the frequency functions can be approximated as

$$\Gamma_{jj} = \frac{1}{\Omega}\frac{\pi}{8\eta\omega_j}; \quad \overline{\Gamma}_{pq} = \varepsilon\sigma^2\Gamma_{pq} \tag{23}$$

The terms related to the coupling, $\Gamma_{jk}$, are not important for a single system, since the $\psi_{jk}=0$.

The power input and the kinetic energy can be written by using the previous relationships and assuming a given spectrum for the excitation, $S_f$:

$$P_{IN} = 2S_f\sum_j 2\eta\omega_j\Gamma_{jj}\psi_{jj}; \qquad \overline{P}_{IN} = P_{IN} \tag{24}$$

$$T = 2S_f\sum_j \Gamma_{jj}\psi_{jj}\psi_{jj}; \qquad \overline{T} = \varepsilon\sigma^2 T \tag{25}$$

For getting finally the mean square velocity:

$$v^2 = \frac{T^{(r)}}{m}; \; \overline{v}^2 = \frac{\overline{T}^{(r)}}{\overline{m}} = \frac{\varepsilon\sigma^2 T^{(r)}}{m\sigma^2} = v^2\varepsilon \tag{26}$$

The simplest choice for the scaling coefficient ε is to consider it equal to $\sigma^2$. Summarizing:

$$\overline{S}_f = S_f \Rightarrow \begin{cases} \overline{P}_{IN}^{(s)} = P_{IN}^{(s)} \\ \overline{T}^{(s)} = \sigma^4 T^{(s)} \\ \overline{A}_{ss} = A_{ss}\sigma^4 \\ \overline{v}^2 = \dfrac{\overline{T}^{(s)}}{\overline{m}} = \dfrac{\sigma^4 T^{(s)}}{\sigma^2 m} = \dfrac{\sigma^2 T^{(s)}}{m} = \sigma^2 v^2 \;\Rightarrow\; v^2 = \dfrac{\overline{v}^2}{\sigma^2} \end{cases} \tag{27-a}$$

$$\overline{S}_f = \sigma^{-2}S_f \Rightarrow \begin{cases} \overline{P}_{IN}^{(s)} = \sigma^{-2}P_{IN}^{(s)} \\ \overline{T}^{(s)} = \sigma^2 T^{(s)} \\ \overline{A}_{ss} = A_{ss}\sigma^4 \\ \overline{v}^2 = \dfrac{\overline{T}^{(s)}}{\overline{m}} = \dfrac{\sigma^2 T^{(s)}}{\sigma^2 m} = v^2 \end{cases} \tag{27-b}$$

Obviously, the choice of ε is not uniquely determined, and infinite combinations of σ and ε could be pursued, but by selecting $\varepsilon=\sigma^2$, one gets that the scaled mean square velocity is equal to the original one and further, the modal overlap factor is kept; generalizing:

$$m_\omega(\omega) = \omega\,\eta(\omega)\,n_\omega; \qquad \overline{m}_\omega(\omega) = \omega\,\overline{\eta}(\omega)\,\overline{n}_\omega = \omega\frac{\eta(\omega)}{\sigma^2}\sigma^2\,n_\omega = m_\omega(\omega) \tag{28}$$

## 4. Estimating the Coupling Loss Factors

### 4.1 Two In-Line Rods

The scaling procedure in terms of the absolute responses was analyzed earlier while here an analysis is presented for determining the coupling loss factors for a given configuration.

All the relevant details for getting the EIC can be found in ref.[5].

The selected structure was composed of two in-line rods (only longitudinal waves are allowed to travel) and the original and scaled responses were assembled by using the standard FEA. At both the ends the structure is clamped.

Figure 5: Configuration of the two rods

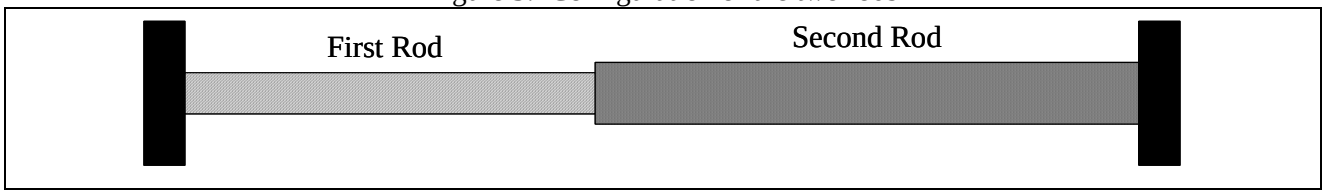


Both the rods are made of the same material: modulus of elasticity, E = 39.476 Pa, mass density, $\rho$ =1 kg $m^{-3}$, longitudinal wave speed, $c_L = (E/\rho)^{1/2}$ = 6.283 m $s^{-1}$. The differences between the two rods are in their lengths and cross-section areas: $L_1 = \pi/3$ m, $L_2 = 2\pi/3$ m, $A_1$ = 1 $m^2$, $A_2$ = 0.4 $m^2$. By using these parameters, a unit global modal density is obtained; in fact: $n_{f1}$ = 0.333 $Hz^{-1}$, $n_{f2}$ = 0.666 $Hz^{-1}$. The odd choice of parameters allows creating a system with a unit total modal density.

The finite element models were built by using as a parameter the number of solution points for each wavelength, NEWL: later this variation will be discussed.

Further, the scaled finite element model has been built by multiplying each coordinate by $\sigma$, the scaling factor, and by imposing an artificial augmented damping, $\overline{\eta} = \eta/\sigma$. This means than the scaled model will have only a fraction of the original degrees of freedom. Generally, the same original mesh could be also kept for the scaled model, but this point will not be addressed here, ref.[6]. Before discussing the results presented in the next pages, it is useful to underline the behaviour of the parameters, $\mu_{jk,}$ that rule the $\Gamma_{jj}$ and $\Gamma_{jk}$ approximations. They are defined as

$$\mu_{jk} = \frac{M_{jk}^2}{1+M_{jk}^2} = \left(\frac{\omega_j \eta_j}{|\omega_j - \omega_k|}\right)^2 \left[1+\left(\frac{\omega_j \eta_j}{|\omega_j - \omega_k|}\right)^2\right]^{-1} \tag{29}$$

Here $M_{jk}$ is the modal overlap between the $j^{th}$ and the $k^{th}$ modes. The scaled ones in the present case are

$$\overline{\mu}_{jk} = \frac{\overline{M}_{jk}^2}{1+\overline{M}_{jk}^2} = \frac{1}{\sigma^2}\left(\frac{\omega_j \eta_j}{|\omega_j - \omega_k|}\right)^2 \left[1+\frac{1}{\sigma^2}\left(\frac{\omega_j \eta_j}{|\omega_j - \omega_k|}\right)^2\right]^{-1} = \frac{M_{jk}^2}{\sigma^2 + M_{jk}^2} \qquad (30)$$

As expected, for σ=1, the scaled system is identical to the original one, while the lower the σ, the higher the differences in terms of frequency distribution[1]. This difference will be reduced by refining the spatial distribution that is by reducing the error of the natural frequencies, and/or enlarging the modal base. In any case, the limiting values for $\mu_{jk}$ are kept; in fact, by considering the modal overlap factor $M_{jk}$ as a continuous variable, Fig.6.

Figure 6: Analysis of the Eq.(31) - $\mu_{jk}$ vs $M_{jk}$ – for several values of the scaling coefficient

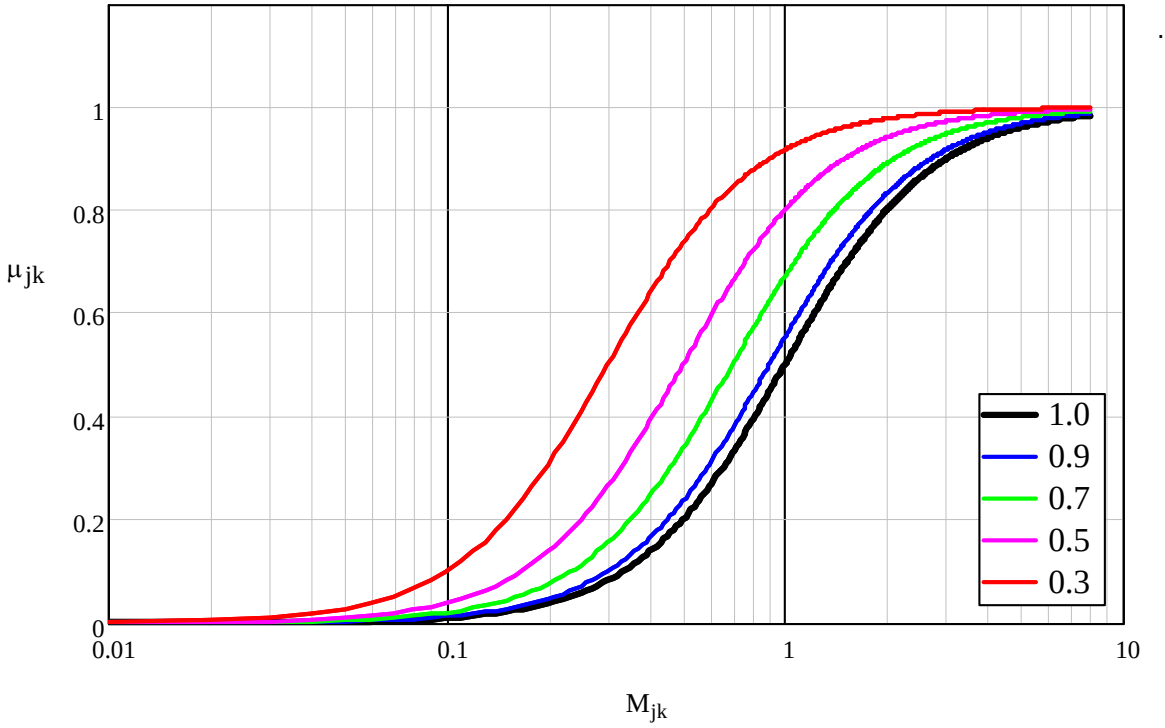


It is evident that $\lim_{M_{jk}\to 0} \mu_{jk}, \overline{\mu}_{jk} = 0$ and $\lim_{M_{jk}\to \infty} \mu_{jk}, \overline{\mu}_{jk} = 1$. Therefore, it is expected that at both very low and very high modal overlap factors, the scaled model will produce the same results as the original model. The main differences are expected in the *intermediate* region (moderate model overlap), and they will be magnified by the scaling coefficient.

It is useful to remember that in standard SEA, the following relationship hold for a generic coupling between the j-th and k-th subsystem:

$$\eta_{jk} n_j \omega = \frac{\tau_{jk}}{2\pi} \qquad (31)$$

[1] It has to be noted that for plate assemblies, the same result is obtained (σ=ε, $\overline{\omega}_j = \omega_j \sigma^{-2}$, $\eta_j = \eta_j \varepsilon^{-1}$), ref.[10].

where $\eta_{jk}$ is the coupling loss factor, $n_j$ is the radian modal density, $\omega$ is the radian excitation frequency, and $\tau_{jk}$ is the transmission coefficient.

From here and for the remaining part of this document, the transmission coefficient will be referred to as the quantity $\tau_{jk}/(2\pi)$.

Figures 7 to 10 contain the results for the present assembly, and they contain: (a) the statistics (mean and variance) of the $\psi_{jj}$ terms for each rod;(b) the original transmission coefficients; (c) the scaled transmission coefficients; (d) the original, scaled and standard coupling loss factors $\eta_{21}$;(e) the original, scaled and standard coupling loss factors $\eta_{12}$; further, the maximum frequency ($f_{max}$), the retained number of original modes (NOM), the retained number of scaled modes (NSM), the number of element for wavelength (NEWL) and the scaling coefficient ($\sigma$) are also indicated, respectively. The x-axis in the figures (b÷e) is the global modal overlap factor.

Figure 7: $f_{max}$=50 Hz, NEWL=5 and $\sigma$=0.5; (a) statistics on original and scaled $\psi_{jj}$; (b) the original transmission coefficients; (c) the scaled transmission coefficients; (d) original and scaled coupling loss factors – $\eta_{21}$; (e) original and scaled coupling loss factors - $\eta_{12}$.

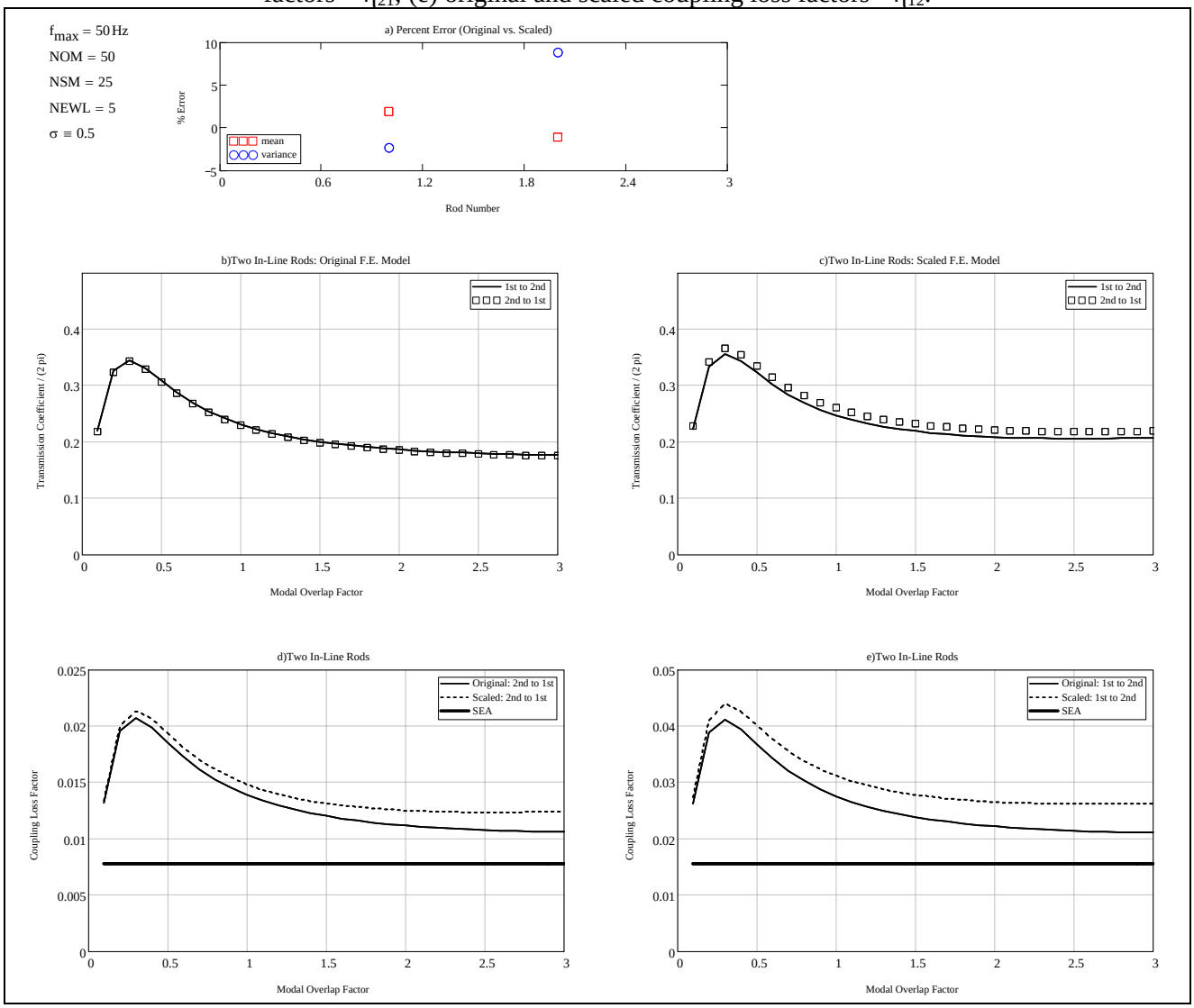

The parameter that is varied is simply the damping, η. The estimation of the coupling loss factor has been based on a band centred at $f_{max}/2$.

Figure 8: $f_{max}$=100 Hz, NEWL=5 and σ=0.5; (a) statistics on original and scaled $\psi_{jj}$; (b) the original transmission coefficients; (c) the scaled transmission coefficients; (d) original and scaled coupling loss factors – $\eta_{21}$; (e) original and scaled coupling loss factors - $\eta_{12}$.

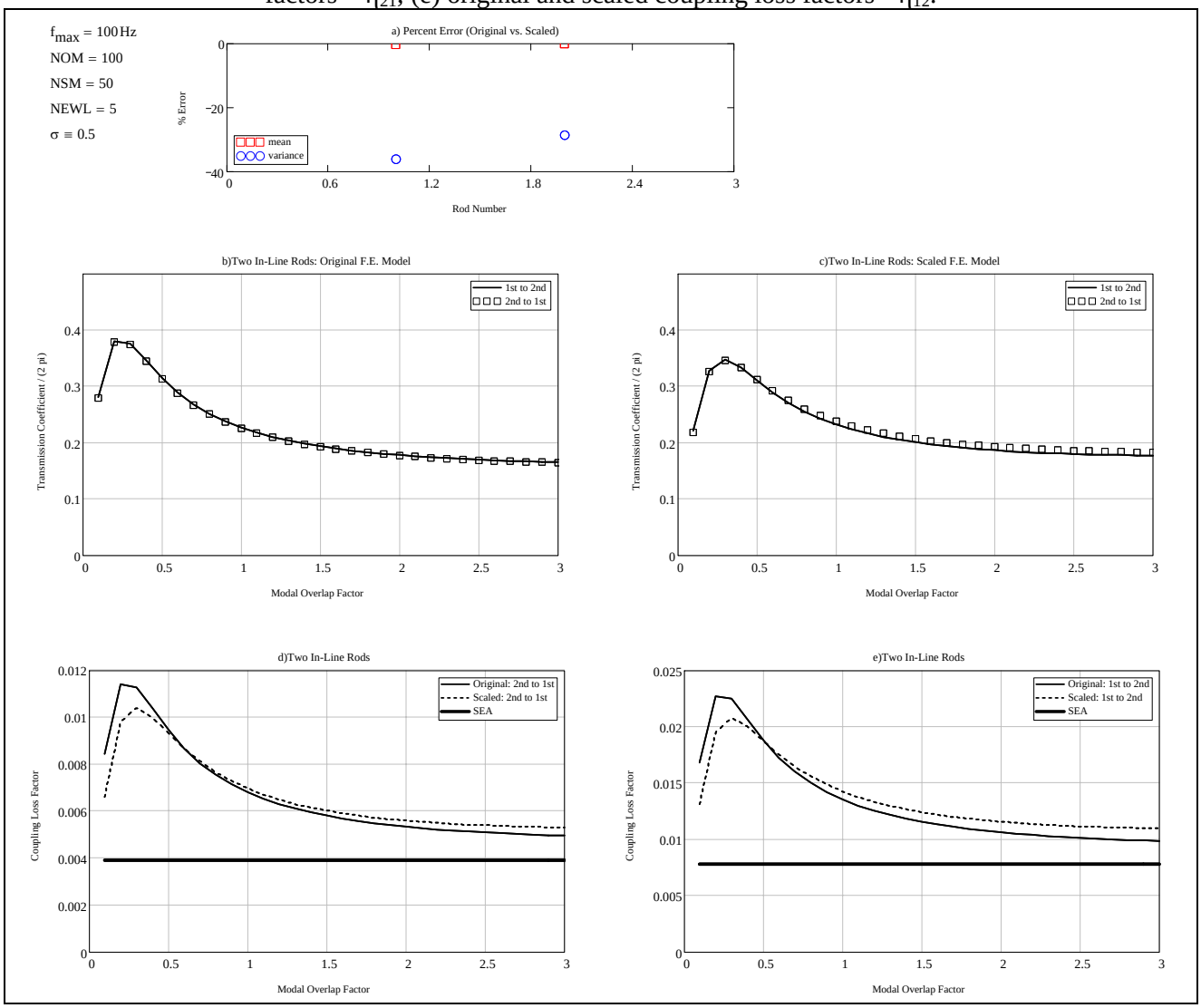


In all the figures, a good estimate of the coupling loss factor $\eta_{12}$ and $\eta_{21}$ has been obtained for very low and very high modal overlap, and the main differences are in the intermediate region, as expected, and some asymptotic values for increasing values of the modal overlap.

Fig.10 and 11 present the effect of increasing the number of modes: the scaled models has σ=0.5 and such an increase improves the accuracy of the prediction of the scaled models.

Fig.12 presents a reduction of the scaling coefficient and it is clear that this is associated with a small degradation of the predictive capabilities in the intermediate region.

The simple doubling of the number of elements per wavelength (NEWL), produce better results since the spatial members, $\psi_{jk}$, are better simulated, Fig.13.

Figure 9: $f_{max}$=100 Hz, NEWL=5 and σ=0.3; (a) statistics on original and scaled $\psi_{jj}$; (b) the original transmission coefficients; (c) the scaled transmission coefficients; (d) original and scaled coupling loss factors – $\eta_{21}$; (e) original and scaled coupling loss factors - $\eta_{12}$.

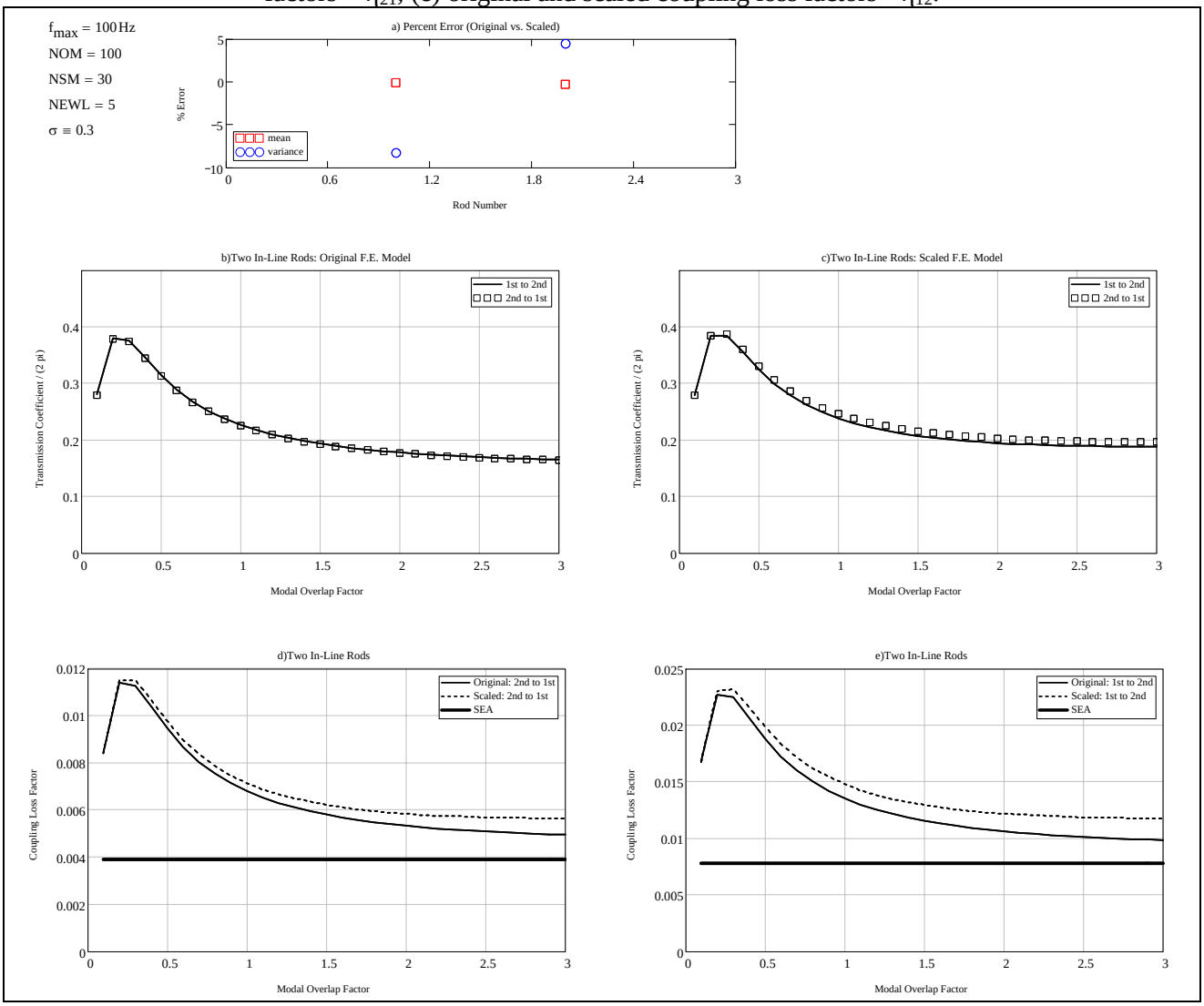


The errors on mean values remain very small and are practically unchanged in all the figures; the analysis of the variances with the number of modes and the scaling coefficient is difficult, even if in general the lower they are the better will be the results.

Figure 10: $f_{max}$=100 Hz, NEWL=10 and σ=0.3; (a) statistics on original and scaled $\psi_{jj}$; (b) the original transmission coefficients; (c) the scaled transmission coefficients; (d) original and scaled coupling loss factors – $\eta_{21}$; (e) original and scaled coupling loss factors - $\eta_{12}$.

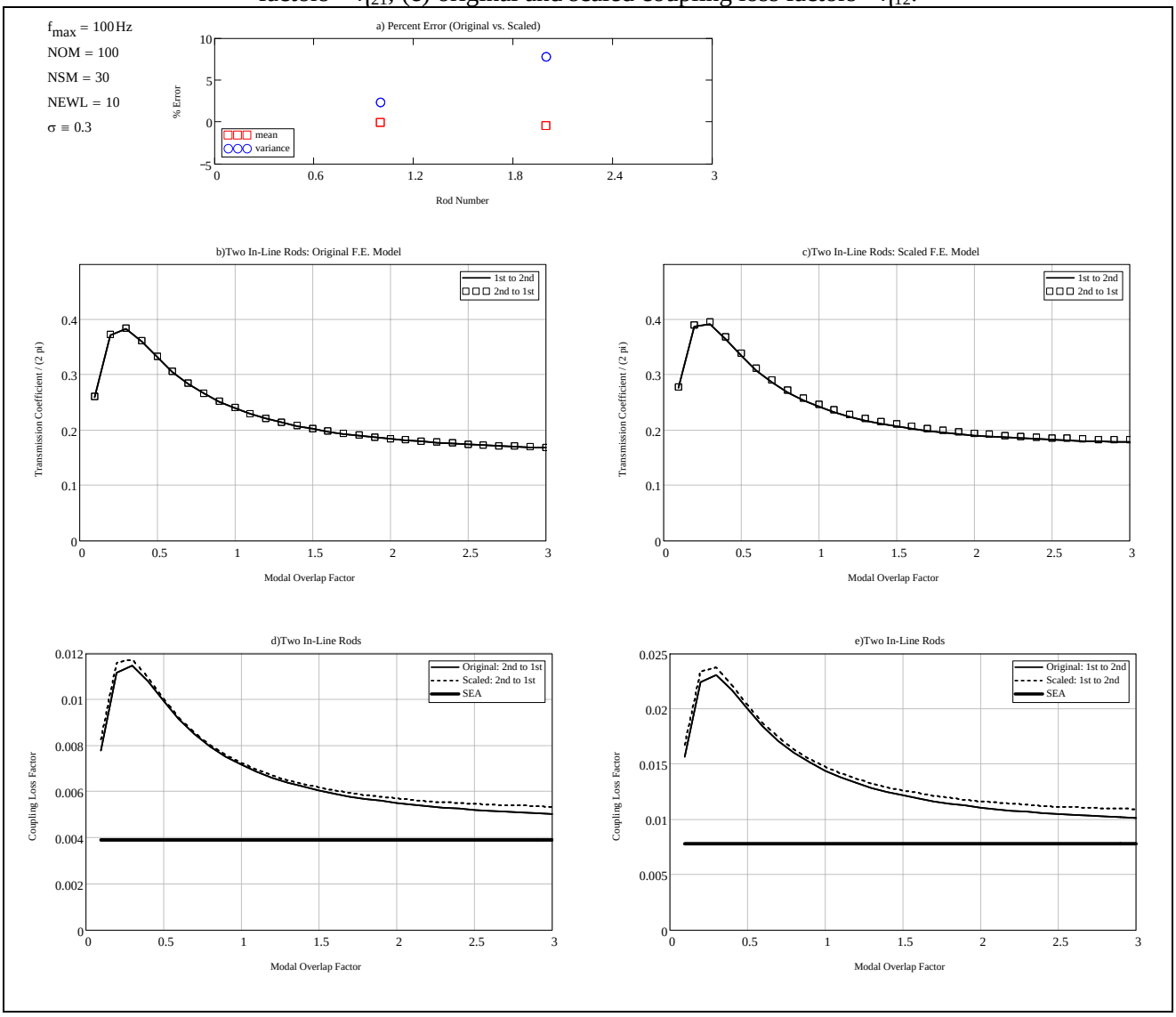

## 4.2 Four In-Line Rods

*4.2.1 First Assembly*

In this case, the assembly analysed in ref.[1] was used for testing the application of the scaling procedure. Again at both the ends the assembly is clamped and all the rods are made of the same material: modulus of elasticity, E = 39.476 Pa, mass density, $\rho$ =1 kg $m^{-3}$. The variations between the four rods are in their lengths and section areas: $L_1$= 0.5171 m, $L_2$ = 0.8885 m, $L_3$ = 0.7072 m, $L_4$ = 1.0288 m; $A_1$ = 1 $m^2$, $A_2$ = 0.4 $m^2$, $A_3$ = 0.9 $m^2$, $A_4$ = 0.6 $m^2$. By using these parameters, a unit global modal density is obtained; in fact: $n_{f1}$ = 0.165 $Hz^{-1}$ , $n_{f2}$ = 0.283 $Hz^{-1}$, $n_{f3}$ = 0.225 $Hz^{-1}$, $n_{f4}$ = 0.327 $Hz^{-1}$.

This configuration is a severe test-case for any energy methods, since it presents the problem of indirect coupling. ASMA was successfully applied to a very similar configuration (six in-line rods), ref.[6].

The results are contained in Figs.(11÷14), where the estimates of the full set of direct and indirect loss factors are presented together with the means and variances of $\psi_{jj}$ for the original and scaled systems. Specifically, the figures contain: (a) the statistics (mean and variance) of the $\psi_{jj}$ terms for each rod; (b) the original direct transmission coefficients; (c) the scaled direct transmission coefficients; (d) the original indirect transmission coefficients; (e) the scaled indirect transmission coefficients.

Figure 11: $f_{max}$=80 Hz, NEWL=5 and σ=0.5; (a) statistics on original and scaled $\psi_{jj}$; (b) original direct transmission coefficients; (c) scaled direct transmission coefficients; (d) direct original transmission coefficients; (e) indirect scaled transmission coefficients.

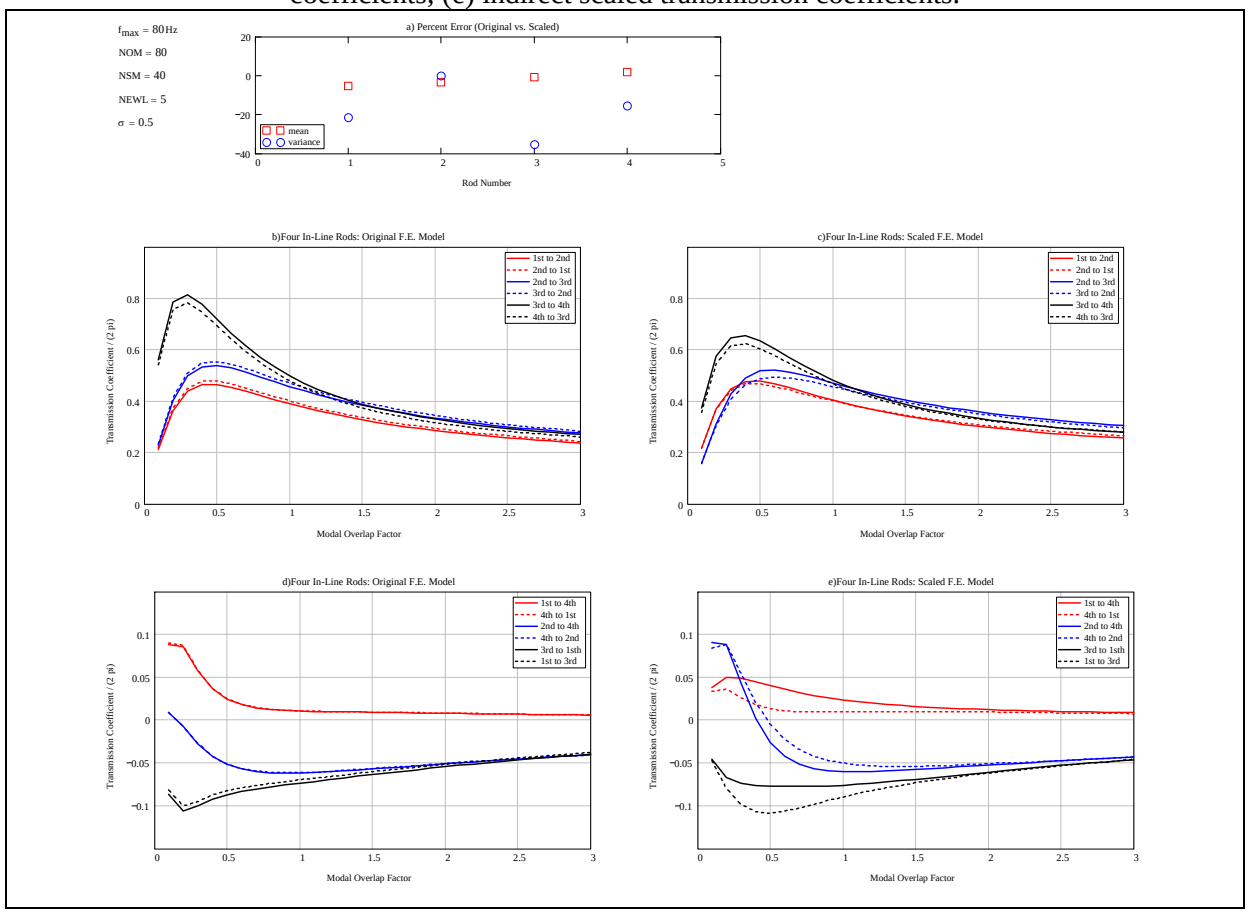

Figures 12 and 13: $f_{max}$=100 Hz, NEWL=5 and σ=0.5 (top) and σ=0.35 (bottom); (a) statistics on original and scaled $\psi_{jj}$; (b) original direct transmission coefficients; (c) scaled direct transmission coefficients; (d) direct original transmission coefficients; (e) indirect scaled transmission coefficients.

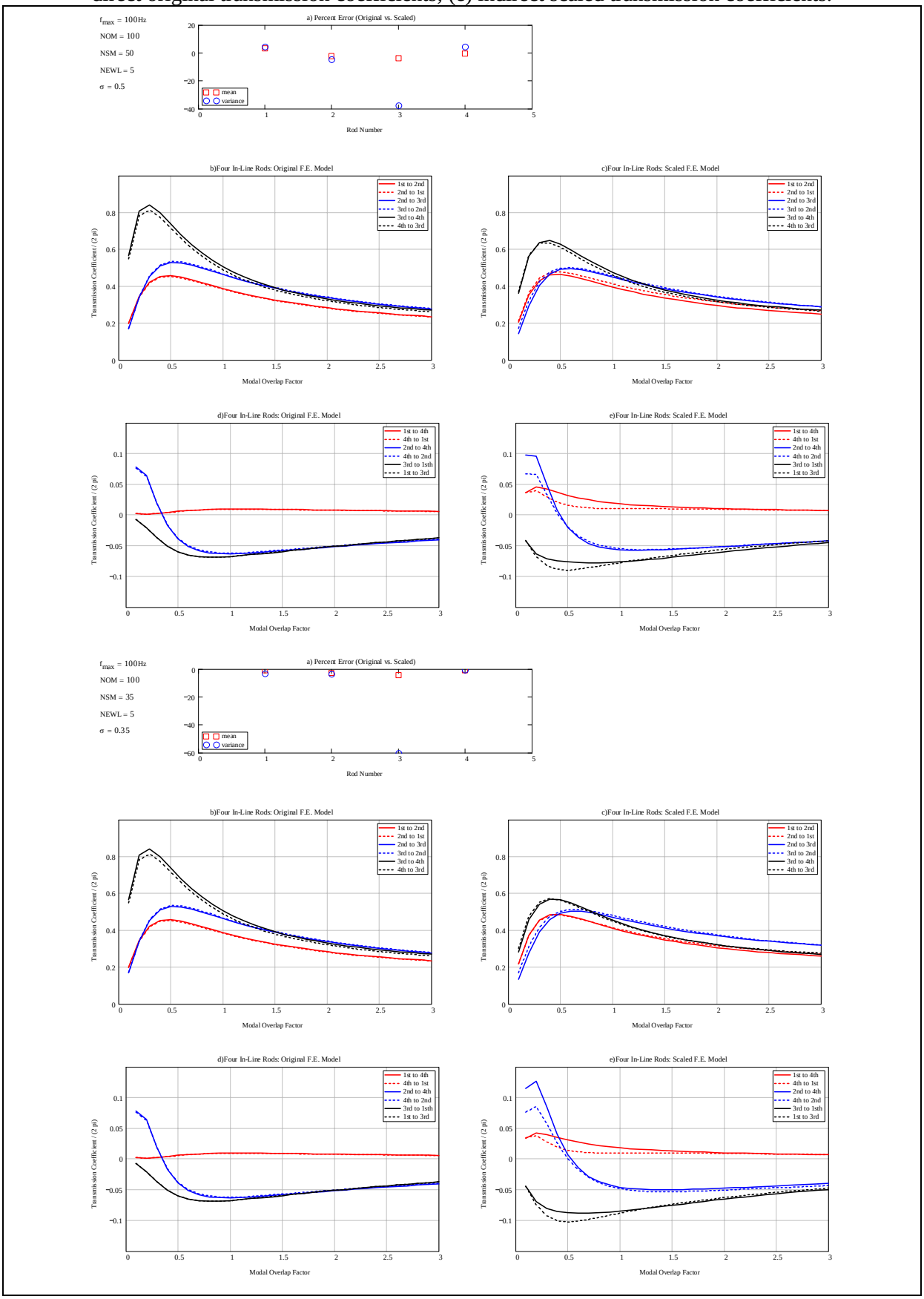

Figure 14: $f_{max}$=100 Hz, NEWL=5 and σ=0.2; (a) statistics on original and scaled $\psi_{jj}$; (b) original direct transmission coefficients; (c) scaled direct transmission coefficients; (d) direct original transmission coefficients; (e) indirect scaled transmission coefficients.

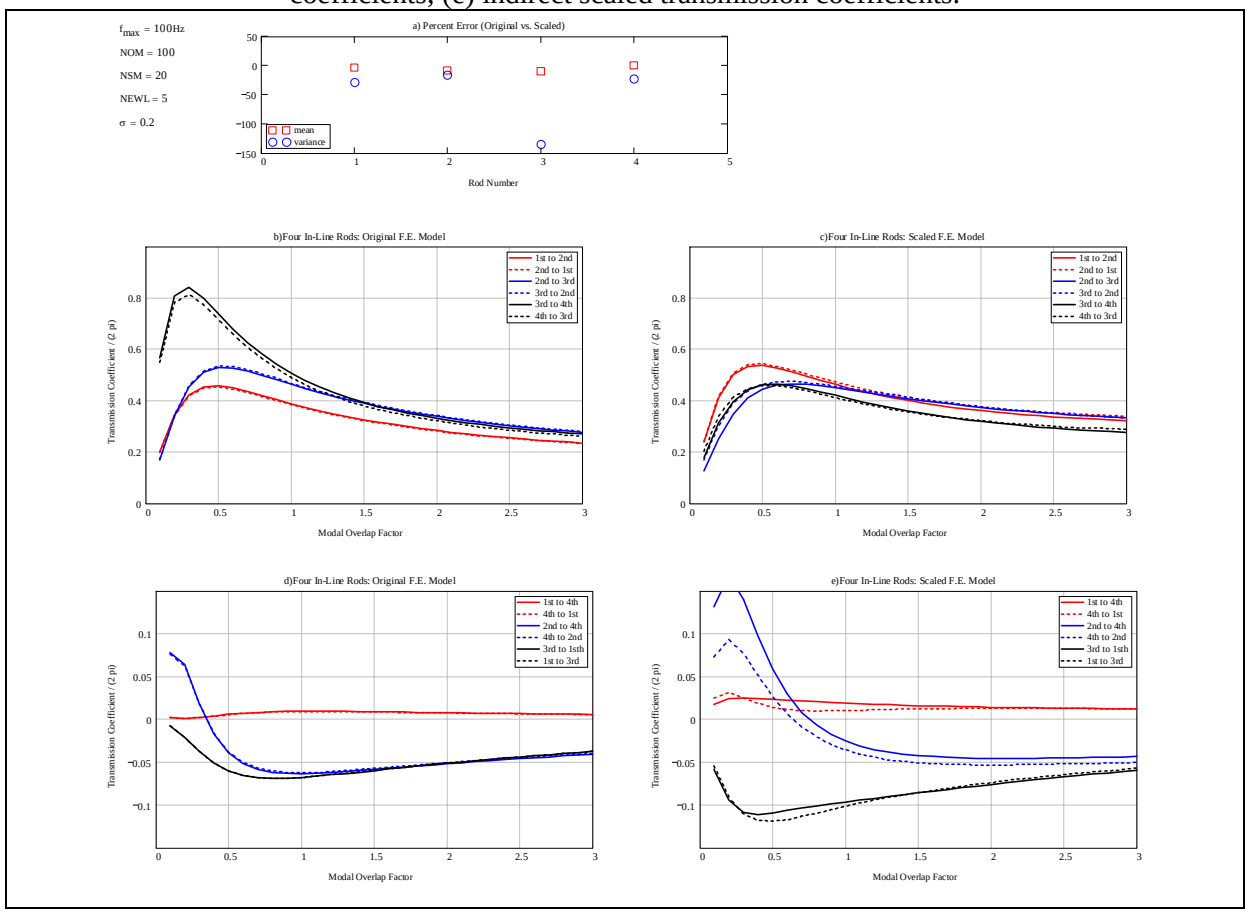


A broad conclusion can be drawn from the present results: ASMA is able to predict the evolution of the full set of direct and indirect coupling loss factors with the modal overlap factors; this can be done according to the proper number of modes for representing the frequency band and the resolution of the spatial information. All the predictions are obtained with a drastic decrease in the computational costs due to both the reduction of the original mesh and the selection of a limited number of scaled modes.

Further investigations are needed for controlling the error on estimating the coupling loss factors as a function of the scaling coefficient and the given number of modes, in order to better quantify an *acceptable approximation level.*

*4.2.2 Second Assembly*

In this case, the analysed assembly was the same as used before; the only variation was in the cross-section areas: $A_1 = 0.6\ m^2$, $A_2 = 1.0\ m^2$, $A_3 = 0.4\ m^2$, $A_4 = 0.9\ m^2$.

The configuration was analysed and presented for the sake of completeness. Results are shown in Fig.15.

Figure 15: $f_{max}$=100 Hz, NEWL=5 and σ=0.5; (a) statistics on original and scaled $\psi_{jj}$; (b) original direct transmission coefficients; (c) scaled direct transmission coefficients; (d) direct original transmission coefficients; (e) indirect scaled transmission coefficients.

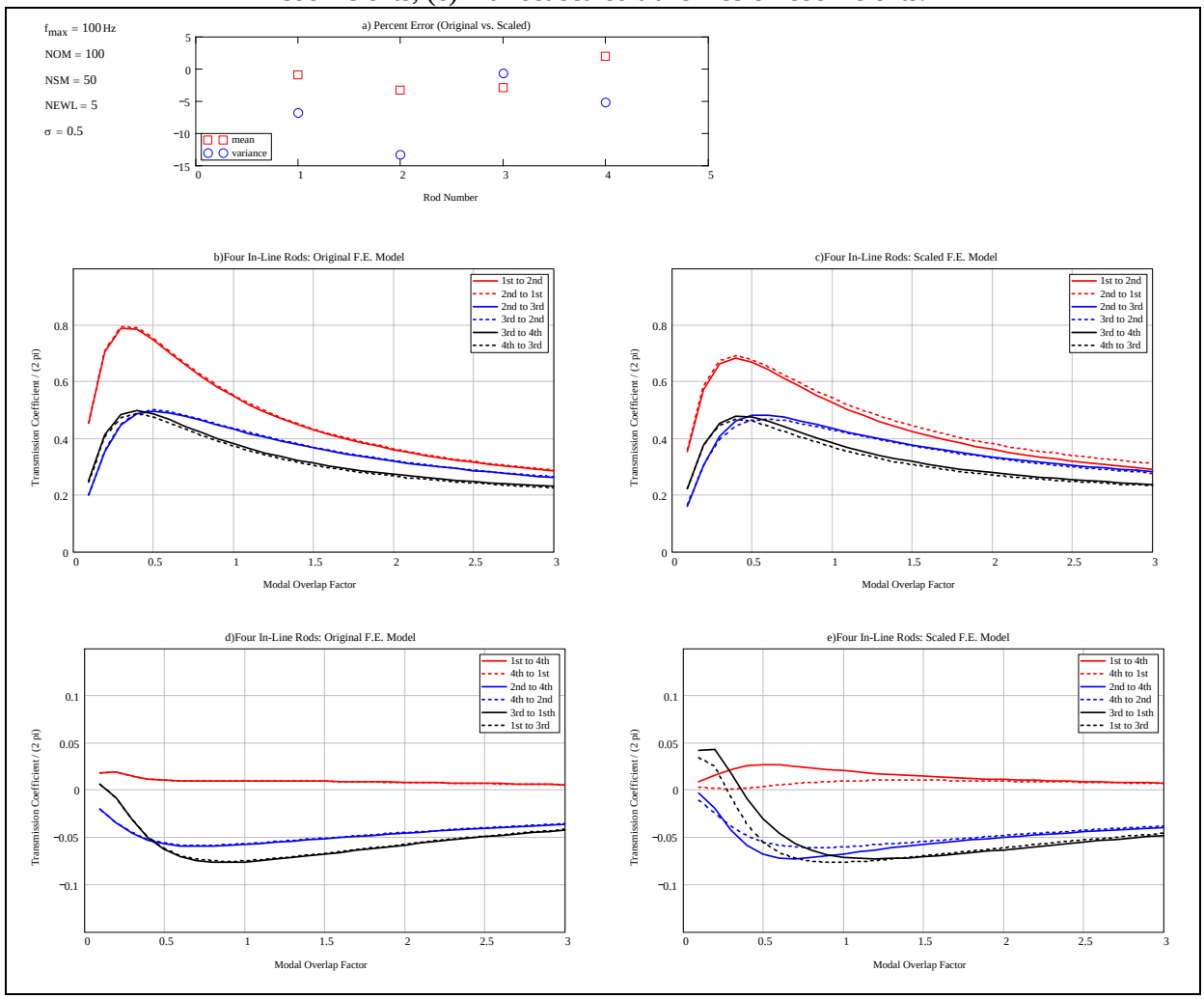

## 5. Concluding Remarks

Some advances have been herein presented concerning the scaling procedure when aimed to the estimation of the coupling loss factors. The possibility of using ASMA (Asymptotical Scaled Modal Analysis) to predict EICs (Energy Influence Coefficients) and coupling loss factors at various values of the modal overlap factor were analysed. Numerical results were presented and they are quite satisfactory even if more work is required.

The Energy Distribution Approach, EDA, furnished a theoretical frame for the overall scaling procedure. The results presented herein have again shown the versatility and computational convenience of ASMA, and it can be directly applied using any finite element solver.

Some points need to be addressed in the future, for gaining more confidence in using ASMA and EIC:

1) Analysis of the error in estimating the coupling loss factors.
2) Analysis of the scaling procedure for the plate assemblies RR, DD and PP, ref.[5].
3) Analysis of the approximations included in ref.[5] when working with the scaling procedure aimed at the estimation of the coupling loss factors.
4) Evaluation of the scaled responses and estimation of coupling loss factors for the configurations where different forms of modal densities are involved (plate + beam, plate + acoustic volume, etc.).
5) Evaluation of the scaled responses and estimation of coupling loss factors for the configurations in which a physical coupling element has to modelled.

In summary, EDA represents a well posed technique aimed at the evaluation of the energy influence coefficients (EIC) that, when appropriately ensemble averaged, can be used to estimate the coupling loss factors used in SEA. It allows the assembling of predictive models at increasing excitation frequency by using a generic modal base. It was herein demonstrated that ASMA can be adopted for such an estimation of the coupling loss factors by using low-cost FEA predictions.

## Acknowledgements

S. DE ROSA was at the Institute of Sound and Vibration Research (ISVR), University of Southampton, from 8 to 22 October 2005, under a grant received from the University of Naples “Federico II” trough a short mobility programme managed by the *Ufficio Programmi Internazionali di Mobilità per Docenti e Studenti*. He was particularly indebted with Dr. A. Thite: the discussions with him were fruitful and precise guides in analyzing the overall procedure.

All the results herein presented were generated by using electronic sheets written in MathCad 12.1; they can be requested directly at the e-mail address, if needed.

## References


[1] Mace B.R.: “Statistical energy analysis, energy distribution models and system modes”, Journal of Sound and Vibration Vol.**264**(2), 2003, pp.391-409.

[2] Mace B.R., Shorter P.J: “Energy Flow Models from Finite Element Analysis”, Journal of Sound and Vibration, Vol.**233**(3), 2000, pp. 369-389.

[3] Mace B.R.: “Statistical Energy Analysis: Coupling Loss Factors, Indirect Coupling and System Modes”, Journal of Sound and Vibration, Vol.**279**, 2005, pp. 141-170.

[4] Lyon R. H.: “Statistical Energy Analysis of Dynamical Systems: Theory and Applications”, The MIT Press, ISBN 0262120712, 1976.

[5] Thite A.N. and Mace B.R.: “Robust Estimation of Coupling Loss Factors from Finite Element Analysis”, ISVR Technical Memorandum 935, University of Southampton, May 2004.

[6] De Rosa S., et alii: “First Assessment of the Energy based Similitude for the Evaluation of the Damped Structural Response”, Journal of Sound and Vibration, Vol. **204**(3) pp.540-548, Dec.1997.

[7] De Rosa S., et alii: “The Random Structural Response due to a Turbulent Boundary Layer Excitation”. Wind and Structures, an International Journal, Vol.**6**(6) Nov. 2003, pp.437-450.

[8] Franco F., et alii: “The Energy based Similitude for the Energetic Vibration Response Prediction of 2D Systems”, Proceedings of the Confederation of European Space Agencies (C.E.A.S.) International Forum on Structural Dynamics and Aeroelasticity, Vol.III, pp.223-229, Rome, 17-20 June 1997.

[9] Martini L., De Rosa S., Franco F.: “The Structural Response of a Three Plate Assembly“, Proceedings of the International Conference on Noise and Vibration Engineering ISMA2004, Leuven (BE), 20-22 September 2004, paper 336.

[10] S. De Rosa, F. Franco, B. R. Mace: “The Asymptotic Scaled Modal Analysis for the Response of a 2-Plate Assembly”, Proceeding of the XVIII AIDAA National Congress, Volterra (PI) - Italy, 19-22 Sep 2005

[11] Cook R. D.: “Concept and Application of Finite Element Analysis”, John Wiley & Sons, ISBN 0471030503, 2nd Ed. 1981.